Journal of the Chinese Chemical Society, **1999**, *46*, 759-770

^{25}Mg NMR Relaxation Study of Mg^{2+}-ATP Complexation in Solutions

Zhi-Shian Shien (沈志賢), Tzy-Jiun Luo (羅滋君) and Lian-Pin Hwang* (黃良平)
Department of Chemistry, National Taiwan University, and Institute of Atomic and Molecular Sciences, Academia Sinica, Taipei, Taiwan, Republic of China.

^{25}Mg NMR relaxation has been applied to characterize the kinetic and dynamic parameters in the complexation process of the Mg^{2+} ion with adenosine triphosphate. A modified linear prediction with singular value decomposition method developed earlier is used to obtain the preliminary chemical shift separation between the free $^{25}Mg^{2+}$ ion and the $^{25}Mg^{2+}$-ATP complex. Then the $^{25}Mg^{2+}$ NMR null point spectra is invoked to find the chemical shift separation and the quadrupolar coupling constant of the complex. With the knowledge of those parameters, T_1 and line width data at 30.62 MHz and 18.37 MHz can be analyzed to determine the correlation times for the fluctuation of electric field gradient at ^{25}Mg and the dissociation rate constants of the complex at the temperature range of 270-320 K. An activation energy of 8.8 kcal/mol for dissociation rate constant is obtained. It is also found that the reorientational motion of the $^{25}Mg^{2+}$-ATP complex is not significantly affected by the formation of ATP aggregates. A similar conclusion is further obtained by comparing the T_1 data of β-^{31}P in ATP and Mg^{2+}-ATP solutions.

INTRODUCTION

The magnesium ion is an important cofactor in the regulation of structure and reactivity of nucleic acids in biochemical processes. The binding of the magnesium ion with adenosine triphosphate (ATP) plays an essential role in the metabolic pathways.[1] NMR methods for studying chemical exchange rely on the study of the temperature-dependent chemical shift variations. The use of ^{31}P-NMR has established a valuable tool for the study of the biological processes in vivo. It was found that the resonance lines of the β-phosphate groups in Mg^{2+}-ATP and in metal free ATP are clearly separated.[2,3,4,5] The use of β-^{31}P chemical shift for studying complexation of Mg^{2+}-ATP should work in principle in a well-defined system, but is not very reliable in a complex biological system influenced by variation of pH, temperature, and ionic strength.[3]

In the present study, ^{25}Mg NMR relaxation was used directly to glean some insight into the nature of chemical exchange in the Mg^{2+}-ATP system. It is well known that the ^{25}Mg chemical shift is very insensitive to the formation of complexes.[6,7,8] Even at low temperature the chemical shift separation between free Mg^{2+} ion and Mg^{2+}-ATP cannot be resolved spectroscopically, but a method based on linear prediction with singular value decomposition and the minimum Euclidean norm condition have previously been developed in our laboratory in attempts to trace the various modes of frequency correlation in the free induction decay.[9,10,11] The usefulness of this method has been verified by applying it to resolve the chemical shifts of ^{25}Mg on binding processes. Subsequently, after taking advantages of the resolved peak separation as a preliminary input to fit the spectra obtained near the null point in an inversion recovery experiment, a successive approximation was applied to find the "exact" chemical shift separation. Here, using the density matrix method with chemical exchange, the complete descriptions of time evolution for longitudinal and transverse relaxation were invoked in the simulation of the spectra observed in inversion recovery experiments.[12-17] ^{25}Mg longitudinal and transverse relaxation data in conjunction with the spectral lines obtained near the null point in an inversion recovery experiment were used to determine the fluctuation correlation times of electric field gradient, the effective quadrupolar coupling constant, and the dissociation rate constants of the Mg^{2+}-ATP complex at various temperatures among 270 and 320 K. Thus, the aim of this work is to characterize the relaxation and kinetic parameters of Mg^{2+}-ATP so that the dynamics of complexation may be revealed from Mg^{2+} NMR study. Discussion is made to examine the effect of ionic strengths on the kinetic process and with the help of ^{31}P T_1 studies, the effects of complex aggregations on ^{25}Mg relaxation is also examined.

THEORY

Exchange Process

In the present system, Mg^{2+} ions are partly bound to ATP

Dedicated to Professor Kung-Tsung Wang on the occasion of his 70th birthday.

and most of the Mg^{2+} in the solution is in a hydrated state. The dissociation and association of Mg^{2+}-ATP complexes, with one metal ion per complex, may be described by the equation[2]

$$Mg^{2+} + ATP \underset{k_{-1}}{\overset{k_1}{=}} Mg^{2+}-ATP \quad (1)$$

where k_1 and k_{-1} are forward and backward rate constants, respectively. In the ^{25}Mg NMR spectrum of such a sample, the ^{25}Mg resonance will be exchanging between the free and metal-bound positions with exchange rates governed by Eq. (1). This exchange may also be viewed as a two-site exchange problem between a slow motion site **s** and a fast motion site **f**, i. e.,

$$f \underset{k_{sf}}{\overset{k_{fs}}{\Leftrightarrow}} s \quad (2)$$

where k_{fs} is the rate constant for transfer from fast site **f** to slow site **s** and k_{sf} is the rate constant from site **s** to **f**, respectively, to represent the exchange process of magnesium nuclei between the free ion state and the bound state in Mg^{2+}-ATP. Clearly,

$$k_{fs} = k_1\left[Mg^{2+}\right] \quad (3)$$

and

$$k_{sf} = k_{-1} \quad (4)$$

Also, the principle of detailed balance demands that

$$[f]k_{fs} = [s]k_{sf} \text{ or } P_f k_{fs} = P_s k_{sf} \quad (5)$$

where P_f represents the equilibrium probability distribution of the **f** site and P_s represents the equilibrium probability distribution of the **s** site. As all other experimental conditions such as pH, ionic strength and temperature are unaltered, it should be noted that k_{sf} remains unchanged and k_{fs} changes with $[Mg^{2+}]$, while the dissociation constant is invariant at equilibrium, i.e.,

$$k_D \equiv \frac{k_{-1}}{k_1} = \frac{k_{sf}\left[Mg^{2+}\right]}{k_{fs}} \quad (6)$$

The equilibrium population at site **s** may be expressed by[16]

$$P_s = \frac{C_{ATP}\left[Mg^{2+}\right]}{C_{Mg}\left\{\left[k_D\right]+\left[Mg^{2+}\right]\right\}} \quad (7)$$

where C_{ATP} and C_{Mg} are the total concentration of ATP and magnesium, respectively. In cases of $[Mg^{2+}] >> k_D$, i. e., the strong association limit for Mg^{2+} with ATP, we have $P_s \cong C_{ATP}/C_{Mg}$. To have a good estimation of binding population following the analysis of null point spectra as will be described in below, one may design the experiments in which the concentrations of $[Mg^{2+}]$ and $[Mg^{2+}$-ATP] in equilibrium, as determined by Eq. (1), may be comparable. This condition can be simply arranged by adding the metal ion to ATP in a given initial concentration ratio.

State Multipoles Representation

A number of mathematical formalisms have been applied to study the relaxation of quadrupolar nuclei. However, the use of state multipoles (statistical tensors) has become popular since the multipole operators transform very simply under rotations and can be associated with multi-quantum coherence, spin order and measurable spectral magnetization.[18] State multipoles are specific linear combinations of the normal density matrix elements. A rank k state multipoles with tensorial component m is defined by,

$$\sigma_m^k = \sum_{\alpha}\sum_{\alpha'} \rho_{\alpha\alpha'}(-1)^{I-\alpha}(2k+1)^{1/2}\begin{pmatrix} I & I & k \\ \alpha & -\alpha' & -m \end{pmatrix} \quad (8)$$

where $\rho_{\alpha\alpha'}$, are density matrix elements and $\begin{pmatrix} I & I & k \\ \alpha & -\alpha' & -m \end{pmatrix}$ is a 3-j symbol.[19,20] It corresponds to k-quantum coherence for m = 1 or -1 and to k-spin order for m = 0 in the case of a multi-spin system with a total spin quantum number I. When k = 1 and m = 0 (or ± 1), σ_m^k corresponds to the longitudinal magnetization (or the transverse magnetization). The advantage of using the state multipoles formalism is that it transforms as a component of the full rotation group. For example, an on resonance radio frequency pulse transforms the state multipoles components according to the relation,[21]

$$(\sigma^+)_m^k = \sum_n D_{mn}^k(\varphi - \pi/2, \theta, \varphi - \pi/2)(\sigma^-)_n^k \quad (9)$$

where θ denotes an θ angle rf pulse with phase angle denoted by φ.

Relaxation Theory and Two-Site Exchange Equation of Motion of Density Matrices

The basic relaxation theory is the same as that used in our previous work,[12,13,15,16] and the relaxation equations were simplified by expressing the spin density matrix with state multipoles.[18] Magnesium ion binding to ATP forms a two-site

Table 1. Relaxation Matrices R and R' for the Quadrupolar Interaction on Resonance, for Quadrupolar Nuclei with Spin-quantum Number I = 5/2. The Notation Follows that of Einarsson and Westlund [23,24]

$$R(or\ \ R) \equiv \frac{1}{125}(\chi)^2 \begin{pmatrix} A & E & 0 \\ E & B & F \\ 0 & F & C \end{pmatrix}$$

	Longitudinal	Transverse
A	$2J_1 + 8J_2$	$3J_0 + 5J_1 + 2J_2 - iQ_1 - 2iQ_2$
B	$1/4\ (82J_1+83J_2)$	$1/24\ (123J_0 + 370J_1 + 497J_2 - 126iQ_1 + 3iQ_2)$
C	$25/4\ (2J_1+J_2)$	$5/12\ (3J_0 + 26J_1 + 16J_2 + 6iQ_1 - 9iQ_2)$
E	$18/\sqrt{14}(J_1 - J_2)$	$27/\sqrt{21}\ (J_0 - J_2 - 2iQ_1 + iQ_2)$
F	$125/(2\sqrt{35})(J_1 J_2)$	$25/12\sqrt{14}\ (3J_0 - 14J_1 - 17J_2 - 6iQ_1 + 3iQ_2)$

[a] The fluctuation of the electric field gradient in the quadrupolar relaxation mechanism is assumed to change in direction but not in magnitude. In the two-site exchange system, the effective quadrupolar interaction χ and the motional correlation time in spectral density functions, J_n and Q_n, are separately redefined for χ_s, χ_f, τ_s and τ_f

[b] The equilibrium value for the longitudinal state multipoles are, $\sigma_0^1 = \frac{\sqrt{35}\gamma_I \hbar B_0}{\sqrt{2}(2I+1)}$ and σ_0^3, $\sigma_0^5 = 0$, where B_0 is the static magnetic field.

system, with the Mg^{2+} ion in exchange between the bulk solution and the binding site of ATP. Here, for ^{25}Mg relaxation in Mg^{2+}-ATP complex, the quadrupolar interaction is considered to be modulated by the reorientational motion of the whole complex while the quadrupolar interaction for the bulk Mg^{2+} ion is modulated by the fluctuation of hydration structure around Mg^{2+} ions.[22] In this work we focus on the magnesium nuclei in Mg^{2+}-ATP that exchanges with the bulk Mg^{2+} ions at a rate that is slow on the molecular correlation time scale that modulates the interaction on quadrupolar nuclei. Thus, the density matrix equation for longitudinal relaxation including exchange between a free site, f and a slowly reorientating site, s, is described by the following rate equation

$$\frac{d}{dt}\begin{pmatrix}\rho_f \\ \rho_s\end{pmatrix} = \begin{pmatrix} -R_f - k_{fs}I & k_{sf}I \\ k_{fs}I & -R_s - k_{sf}I \end{pmatrix}\begin{pmatrix}\rho_f \\ \rho_s\end{pmatrix} \qquad (10)$$

where I is a unit matrix, k_{fs} represents the microscopic rate constant for transfer from site **f** to site **s** and k_{sf} represents the microscopic rate constant from site **s** to **f**. Also $\boldsymbol{R}_s$ (or $\boldsymbol{R}_f$) is the Redfield relaxation matrix, as listed in Table 1, for the longitudinal components of the state multipoles in site **f** (or **s**).[17] Here k_{fs} and k_{sf} are assumed *a priori* to be the same as macroscopic rate constants used in Eq. (2). The column density matrices ρ_f and ρ_s are defined as column density matrices of state multipoles in site **f** and **s**, respectively, by $\tilde{\rho}'_f = [(\sigma_0^1)_f, (\sigma_0^3)_f, (\sigma_0^5)_f]$ and $\tilde{\rho}'_s = [(\sigma_0^1)_s, (\sigma_0^3)_s, (\sigma_0^5)_s]$. To guarantee that the state multipoles achieve thermal equilibrium values at infinite time, the difference between σ_0^k and its equilibrium value is substituted into Eq. (10). Similarly, the transverse relaxation equation modified to include exchange is defined by,

$$\frac{d}{dt}\begin{bmatrix}\rho'_f \\ \rho'_s\end{bmatrix} = \begin{bmatrix} -R'_f - k_{fs}I - i(\omega_0 - \delta_f)I & k_{sf}I \\ k_{fs}I & -R'_s - k_{sf}I - i(\omega_0 - \delta_s)I \end{bmatrix}\begin{bmatrix}\rho'_f \\ \rho'_s\end{bmatrix} \qquad (11)$$

where ω_0 is the Larmor frequency, δ_f and δ_s are the chemical shifts of magnesium nucleus at the fast and slow sites, respectively. R'_f (or R'_s) is the Redfield relaxation matrix, as listed in Table 1, for the transverse components of the state multipoles in site **f** (or **s**).[17,23,24] Unlike the longitudinal relaxation matrices, which are real, the transverse relaxation matrices are complex. The real parts cause the relaxation rate and the imaginary parts give rise to the dynamic frequency shift. The column density matrices are defined by $\tilde{\rho}'_f = [(\sigma_1^1)_f, (\sigma_1^3)_f, (\sigma_1^5)_f]$ and $\tilde{\rho}'_s = [(\sigma_1^1)_s, (\sigma_1^3)_s, (\sigma_1^5)_s]$. It should be noted that Eqs. (10) and (11) apply for both density matrix and state multipoles formalisms. In order to guarantee the validity of Eqs. (10) and (11) the condition $\tau_{ex} >> \tau_s$ must hold. Here we defined τ_{ex} as $\tau_{ex} = P_s / k_{fs} = P_f / k_{sf}$

and τ_s as the correlation time for the fluctuation of electric field gradient at **s** site. In the slow exchange limit the condition $|\delta_s - \delta_f|\ \tau_{ex} >> 1$ holds.

Simulation of Null Point Spectra

The use of the above theory in simulating the free induction decay for two-site exchange in the inversion-recovery experiment will be described here. Null point spectra are merely those spectra acquired at τ delays such that the net magnetization is near 0. The equilibrium state multipoles can be calculated from the corresponding density matrix elements to be[17]

$$(\sigma_0^1)_{eq} = \frac{\sqrt{35}\gamma\hbar B_0}{\sqrt{2}(2I+1)kT}$$

$$(\sigma_0^3)_{eq} = 0 \text{ and } (\sigma_0^5)_{eq} = 0 \qquad (12)$$

where B_0 is the external field and I=5/2 is the total nuclear spin quantum number of the ^{25}Mg nuclei. Since we have exchange species, the individual multipole must be appropriately population weighted. The effects of the π pulse were then calculated. Thus immediately after the π pulse and including population weighting the state multipoles are $(\sigma_0^k)_{f(s)} = -p_{f(s)}(\sigma_0^k)_{eq}$, where $(\sigma_0^k)_{eq}$ is the equilibrium state multipoles. Eq. (10) is then used to follow the evolution of the longitudinal magnetization and the "motional" behavior of the spins during the delay τ. Then, following the physical significance of Eq. (9) the $\pi/2$ pulse transforms the longitudinal state multipoles into transverse state multipoles. The rf pulses are considered to be delta functions and so do not cause mixing of the site **f** and site **s** multipoles. The effects of the $\pi/2$ pulse were calculated, and the result formed the initial condition for calculating the evolution of transverse magnetization during the acquisition period using Eq. (11). The time evolution of the following term $\left[(\sigma_1^1)_f + (\sigma_1^1)_s\right]$ corresponds to the free induction decay. The spectral line shape is related to the real part of the Fourier-Laplace transform of this term, which evolves during the acquisition period.

Evaluation of Spectral Line Width

The calculated free induction decay and the spectrum after a $\pi/2$ pulse may be obtained from the time evolution of $\left[(\sigma_1^1)_f + (\sigma_1^1)_s\right]$ following the transverse relaxation expressed by Eq. (11). For this case the equilibrium distribution accounted for the initial conditions of transverse multipoles, i.e., $\left(\sigma_1^k\right)_{f(s)} = P_{f(s)}\left(\sigma_0^k\right)_{eq}$. Since the spectral lines obtained in an exchange process may not be Lorentzian, the full widths at half height (denoted by $\Delta\nu_{1/2}$) and at one-third height (denoted by $\Delta\nu_{1/3}$) were both used in the evaluation of exchange data in order to correctly reflect the contribution of a slow component in the shoulder part of the spectral line.

Evaluation of Longitudinal Relaxation Time

Simulation of ^{25}Mg longitudinal relaxation measurements derived from the system with two-site exchange was in essence the same as that for evaluating the null point spectra. The intensity of the spectral line obtained from the term $[(\sigma_0^1)_f + (\sigma_0^1)_s]$ with τ delay in the inversion-recovery experiment was used to represent the magnetization for longitudinal relaxation. The net magnetization derived from this was well described by a single exponential with time constant T_1.

EXPERIMENTAL

^{25}Mg obtained as 94.5% ^{25}MgO from Cambridge Isotope Laboratories was dissolved in metal-free hydrochloric acid and neutralized to a final pH of 7.4 with NaOH prepared in D_2O solutions. Tris(hydroxymethyl)-aminomethane, tris(hydroxymethyl)aminomethane hydrochloride and the disodium salt of ATP (Grade II) were purchased from Sigma MO. D_2O was purchased from Isotect OH. Other chemicals were of guaranteed grade and used without further purification. The ^{25}Mg NMR measurements were performed on Bruker MSL-500 and MSL-300 spectrometers operating at 30.62 and 18.37MHz, respectively. Transverse relaxation measurements were obtained from line width at half height and at one-third height. The null point spectra and longitudinal relaxation measurements were obtained using the inversion-recovery pulse sequence. ^{25}Mg NMR null point spectra were acquired only at 30.62 MHz. Typical ^{25}Mg acquisition parameters were a spectral width of 30 kHz, digitized into 4K data point with a $\pi/2$ pulse length of about 20 μs, and NS = 30000. A decay of at least 10 T_1 was allowed between scans for the T_1 and null point spectra. The temperature was controlled within ± 0.1 ℃ and was calibrated with a methanol reference. There is an ~ 8% error

Table 2. Temperature-dependent Spin-lattice Relaxation Time and Motional Correlation Time for f Site, Dissociation Rate Constant, Reorientational Correlation Time of Mg^{2+}-ATP Complex, and Measured Viscosity at Different Temperatures

Temp/K	270	275	280	285	290	300	310	320
T_{1f} (ms)[a]	52.2	63.3	78.1	93.8	105.3	130.4	160.4	190.7
τ_f (ps)[b]	10	8.0	6.4	5.3	4.6	3.8	3.3	2.8
k_{-1} (s^{-1})[a]	643	1100	1500	2000	2800	4300	6500	10000
τ_s (ps)[b]	1600	1350	1090	900	690	530	390	300
η (mPas)[c]	(3.97)	3.26	2.66	2.28	1.74	1.42	1.07	0.878

[a] Values have a 8% error associated with them. [b] Values have a 6% error associated with them. [c] Values have a 1.5% error associated with them. Viscosity at 270 K was obtained by extrapolation data above 270 K.

associated with the T_1 measurements and a ~ 10% error associated with the line width measurements.

NMR samples with various ATP concentrations for ^{25}Mg measurement (Sample A : 40 mM, B : 30 mM, C : 20 mM and D : 10 mM) were prepared by dissolving Tris, Tris-HCl, and ATP in D_2O to give Tris 0.18 M, Tris-HCl 0.78 M and Mg^{2+} 100 mM. Ionic strength for samples B, C and D were adjusted with $NaClO_4$ to give the same ionic strength (1.38 m) as in sample A. The pH values of final solutions were about 7.4 at room temperature. Prior to NMR measurement, each solution was bubbled with nitrogen for 3 min to remove dissolved oxygen and then immediately flame sealed inside 10-mm NMR tubes. Samples of various ATP concentrations ([ATP] : 20 mM, 10 mM, 8 mM, 5 mM) with / without Mg^{2+} for ^{31}P measurement at 298 K and 11.75 T (202.46 MHz) were prepared in the same way, but with different ionic strength (0.12 m). Here, for a sample containing Mg^{2+}, the concentration of ATP is twice the Mg^{2+} concentration.

Temperature-dependent viscosity of sample A with normal Mg^{2+} salt was determined using an Ostwald viscometer with deionized water as reference at respective temperature.[25]

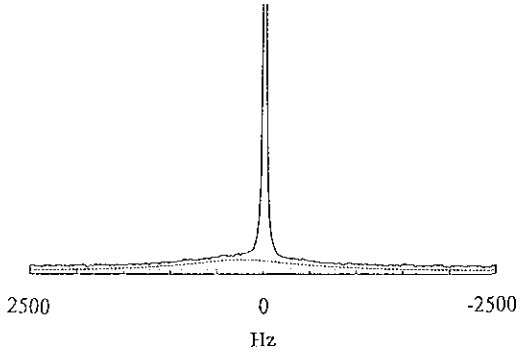

Fig. 1. ^{25}Mg spectrum obtained in an aqueous solution of sample D at pH 7.4 containing 100 mM Mg^{2+} and 10 mM ATP at 270 K and 30.62 MHz on a Bruker MSL-500 Spectrometer. The initial 256 data points in the FID were used in the analysis of spectral lines. The two resolved resonance expressed in dashed lines corresponding to the Mg^{2+}-ATP (broad line) and free Mg^{2+} (sharp line) states, respectively. Other parameters used are NS=75000, DW=5 μs, and D3=20 μs. The [Mg^{2+}]/[Mg^{2+}-ATP] ratios after corrections for the effect of initial dead time relaxation was 9.02/1.

RESULTS

Determination of Relaxation Parameters for Free Site of Mg^{2+} Ion

In subsequent data analysis it was assumed that the value of the electric field gradient at the qradrupolar nuclei was independent of temperature and that only the direction of electric field gradient altered. The quadrupolar coupling constant for free Mg^{2+} ion was taken from ^{25}Mg nuclear quadrupolar resonance spectra of $MgCl_2 \cdot 6H_2O$ measured at 77 K.[26] It yielded a quadrupolar coupling constant and asymmetry parameter of 1477 kHz and 0.20, respectively. It corresponds to an effective quadrupolar coupling constant χ_f = 1487 kHz. ^{25}Mg T_1 values, measured in the solution containing the same composition as in samples A without ATP, was used to evaluate the correlation time for the fluctuation of electric field gradient at f site (τ_f) as listed in Table 2 according to

$$\frac{1}{T_{1f}} = \frac{3\pi^2}{10}\left(\frac{2I+3}{I^2(2I-1)}\right)\chi_f{}^2\tau_f \qquad (13)$$

where the motional narrowing condition is imposed and χ_f is in Hz.

Estimation of Chemical Shift Separation and Determination of Relaxation Parameters from Null Point Spectral Analysis

At 270K the formation of a Mg^{2+}-ATP complex in solution was observed as a single resonance line. It has been shown that at this temperature Mg^{2+} forms a 1 : 1 complex with ATP in aqueous solution.[27] The dissociation constant of [Mg^{2+}-ATP] has been measured by several methods, notably by the temperature-jump method. It yielded $k_D = (k_{-1}/k_1) = 10^{-(4\pm0.5)}$ M at 298 K[28] with ionic strength 0.1 m. In all the samples involved in this work, the most dilute [Mg^{2+}] concentration estimated was [Mg^{2+}] = 60 mM. The error occurred in applying $P_s = C_{ATP}/C_{Mg}$ from Eq. (7) which can be calculated to be less than 0.5% at 298 K. Since the dissociation constant decreases slightly with temperature, the approximation is valid over the temperature range studied here.

^{25}Mg spectra for deconvolution were obtained with NS = 75000 for sample D (10 mM ATP) and null point spectra were conducted with NS = 30000 for sample A (40 mM ATP) at 270 K and 30.62 MHz. From theoretical calculation, the choice of the sample with low complex concentration leads to a larger separation of resolved chemical shifts. In order to resolve the slow component, the use of the most concentrated ATP sample for null point spectral analysis is needed.

As in our previous work, chemical shift separation was estimated from tracing the frequency correlation in the free induction decay[11] according to the analysis based on the modification of linear prediction with singular value decomposition method. For sample D (10 mM ATP) at 270 K the resolved spectra were shown in Fig. 1 in which the broad peak was assigned to the bound $^{25}Mg^{2+}$ resonance. The spectral intensity for free and bound magnesium ions after correction for the initial dead time was 9.02:1 which agrees excellently with a stoichiometric estimation. This

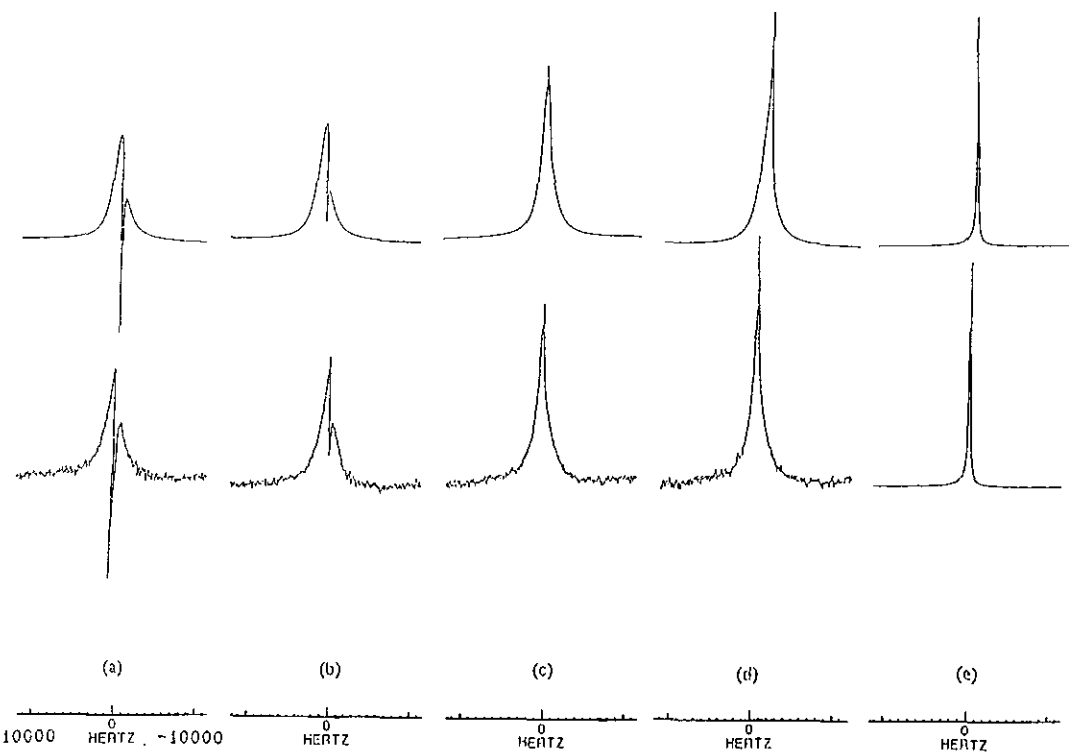

Fig. 2. Simulated (top) and experimental (bottom) ^{25}Mg inversion recovery spectra for sample A near the null point as a function of the delay τ. The observed line width when the τ delay was sufficient to ensure full relaxation was 195 Hz. The τ values and ordinate-magnifying values for the spectra are given respectively by (a) 1.65 ms, 16; (b) 1.75 ms, 16; (c) 1.85 ms, 16; (d) 1.90 ms, 16; (e) 10 ms, 1. The spectra were simulated using Eqs. (9), (10) and (11) with quadrupolar coupling constants χ_f = 1487 kHz and χ_f =3600 kHz and fluctuation correlations times of the electric field gradient of τ_f = 10 ps and τ_s = 1600 ps and LB = 25 Hz was used to account for the line broadening in experiment and simulation.

was also confirmed by the fact that the intensity of the broad component varies linearly with ATP concentration presented in samples A, B and C. Thus, an estimated 9.9 ppm was obtained as the observed peak separation between free and bound magnesium state at 270 K. This value was taken as the first approximation for chemical shift difference in the fitting of null point spectra. Then taking the obtained k_{-1}, and increasing the magnitude of chemical shift separation, a successive approximation has been applied to confirm the same observed peak separation (9.85 ppm) for sample D at 270K with the final convergent parameters, e.g., χ_s = 3600 kHz, τ_s = 1600 ps, k_{-1} = 643 s^{-1} and $|\delta_s - \delta_f| = 10.8$ ppm. The null point spectra of sample A together with their corresponding simulations are shown in Fig. 2.

Longitudinal Relaxation and Transverse Relaxation of Mg^{2+} Ions in ATP Solutions

^{25}Mg longitudinal relaxation measurements were conducted on samples at various temperatures and at 18.37 MHz and 30.62 MHz. The nonexponential transverse relaxation is evident from the non-Lorentzian line shape due to slow exchange process, especially for samples at lower temperature. Therefore, in addition to the usual line width measurement ($\Delta\nu_{1/2}$) at half height, the line width at one-third height ($\Delta\nu_{1/3}$) is also employed to analyze the data. The calculated and experimental T_1 and line widths are shown in Figs. 3-5 for comparison.

Determination of the Dissociation Constants at Various Temperatures

The longitudinal relaxation and line width measurement at 18.37 MHz and 30.62 MHz for samples A, B, C, and D were performed at a temperature range from 270 to 320 K. The longitudinal relaxation times T_1 were calculated as described in Sec. 2.6.

The determined χ_s and χ_s along with temperature-dependent τ_f values were used as inputs in the evaluation of k_{-1} and τ_s at various temperatures. Experimental T_1 and line widths at half height and one-third height were utilized in the data analysis. It was found that within the experimental error the same set of data can fit all A, B, C and D samples, at a given temperature. The results are shown in Figs. 3-5. The correlation time for the fluctuation of quadrupolar interaction at site **s**, τ_s, and the dissociation rate

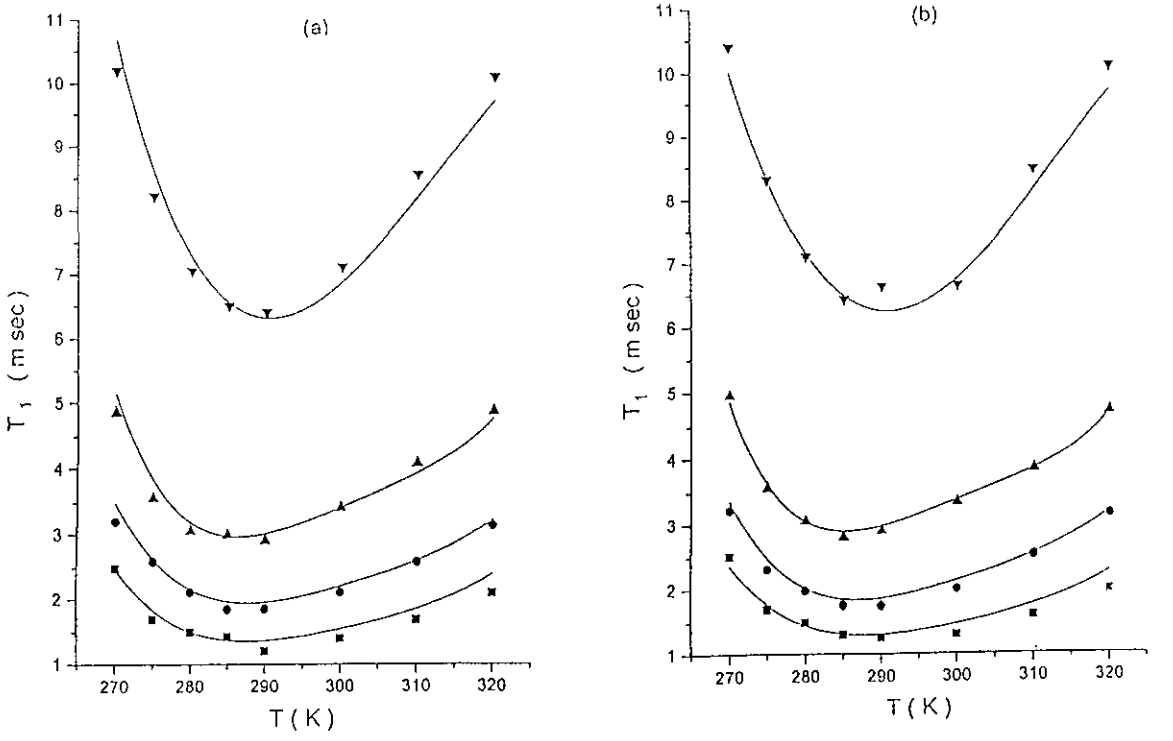

Fig. 3. Experimental and calculated ^{25}Mg spin-lattice relaxation rates as a function of temperature. (■), (●), (▲) and (▼) are measured T_1 data for samples containing 40 mM, 30 mM, 20 mM and 10 mM ATP, respectively, at (a) 30.62 MHz and (b) 18.37 MHz.

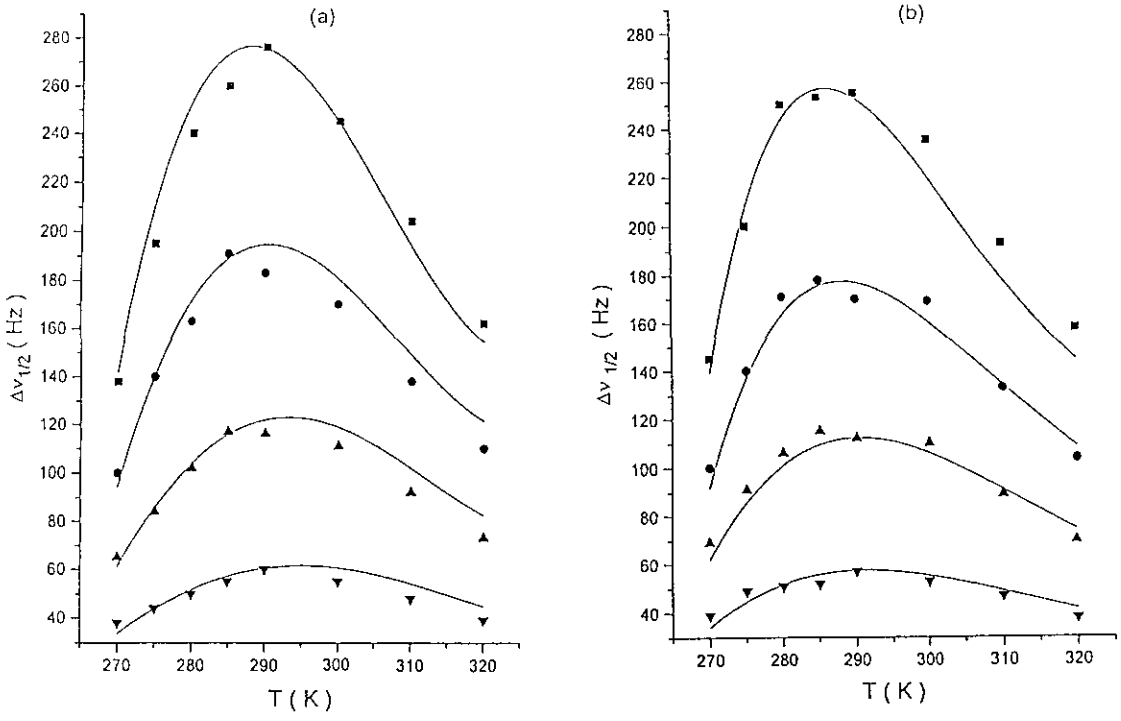

Fig. 4. Experimental and calculated ^{25}Mg full line width at half height $(\Delta\nu_{1/2})$ for samples A (■), B (●), C (▲) and D (▼) as a function of temperature at (a) 30.62 MHz and (b) 18.37 MHz.

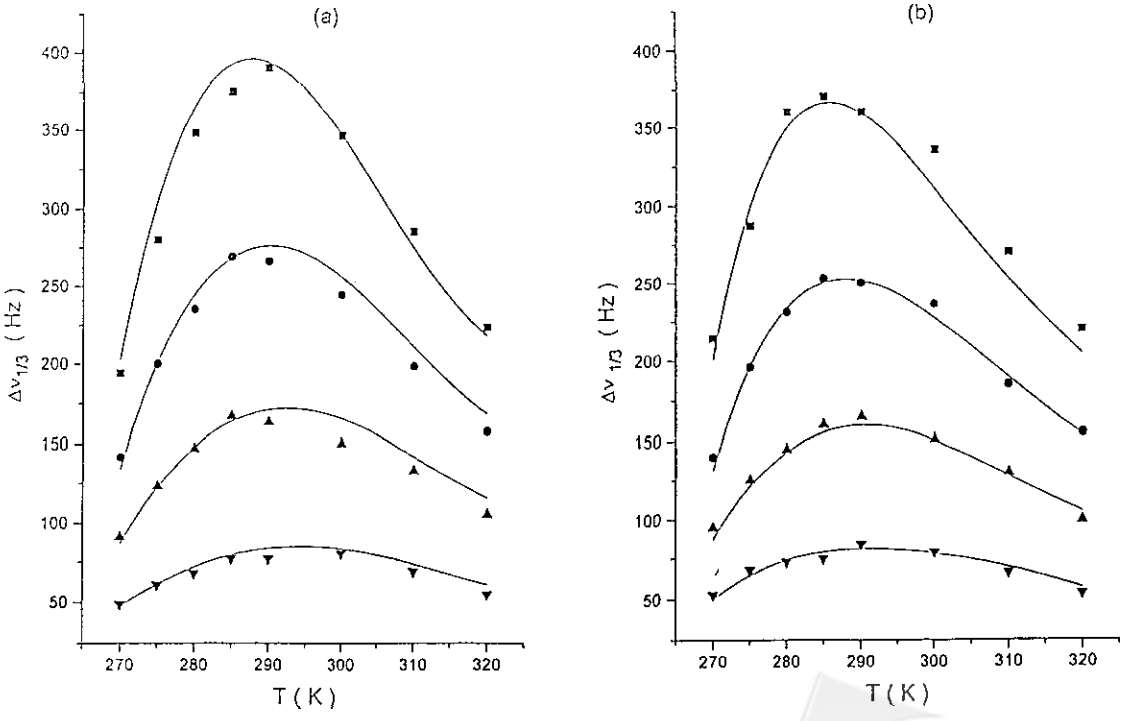

Fig. 5. Experimental and calculated ^{25}Mg full linewidth at one-third height for sample A (■), B (●), C (▲) and D (▼) as a function of temperature at (a): 30.62 MHz and (b): 18.37 MHz.

Table 3. ^{31}P Spin-lattice Relaxation Time of β-Phosphate in ATP and ATP-Mg^{2+} D_2O Solutions with Ionic Strength 0.12 m at 298K and a Resonance Field of 11.75 T and at 7.05 T as Shown in Parenthesis

ATP(mM)	Mg^{2+}(mM)	T_1(sec)[a]
20	10	0.20 (0.22)
10	5	0.23 (0.24)
8	4	0.28 (0.25)
5	2.5	0.31 (0.31)
20	0	0.18
10	0	0.21
8	0	0.24
5	0	0.27

[a] 8% error has been associated with T1, measurement

rate constant used in fitting experiments are listed in Table 2.

DISCUSSION

Compared to previous studies of magnesium ion binding to ATP, no detailed relaxation theory was applied to the analysis of previous experiments. The present study used the complete relaxation theory to simulate the spin relaxation data and, in particular, the null point spectra in an exchange system. The physical origin of the usual null point spectra reported previously was related to the effect of the third rank multipoles for quadrupolar nuclei with $I \geq 3/2$[17]. However, the null point spectra as displayed in Fig. 2 were the consequence of two different relaxing species in the slow exchange regime. The quadrupolar nuclei undergo exchange between a site **f** in the extreme narrowing condition and a site **s** near the dispersion region. Thus, the component at site **f** relaxes much slower than that at site **s**. The line shape of the **s** component was figured out from the spectral shoulder region. The complex formation between Mg^{2+} and the triphosphate anion resulted in a larger electric field gradient than that at the free Mg^{2+} ion. Therefore, this effect along with the slow reorientational motion of the complex gave rise to the broadening of the spectral line for site **s**. Here we refrained from attempting to calculate χ_s since a number of important parameters were not known.[29] As pointed out by Rose and Bryant,[30] the absence of covalent bonds between the exchanging ion and the binding site also complicates the interpretation of χ_s.

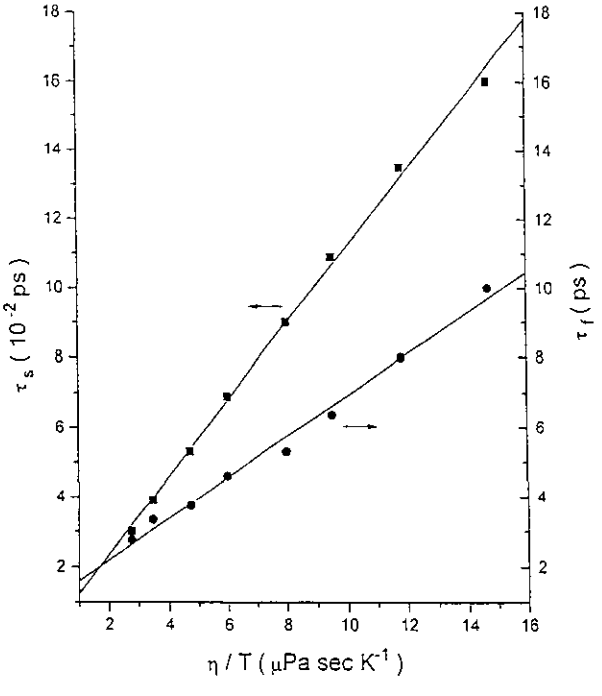

Fig. 6. Fluctuation correlation times of electric field gradient at free Mg^{2+} site and Mg^{2+}-ATP binding site as a function of η/T. The straight lines are the results from linear regression of the data with slope 111000 and 600 ps K/(mPa s) for s site and f site respectively.

The fitting of observed spectra from null point measurement with those calculated is based upon the line shape, appearance time, and intensity of null point spectra relative to the fully relaxed spectrum. Line shape of the null point spectra contains information complementary to normal longitudinal and transverse relaxation measurements. Also the position of fine structure that shows up in (a) and (b) of Fig. 2 is sensitive to the value used for chemical shift separation between component spectra as the other parameters are fixed.

Fig. 3 shows the temperature dependence of the observed ^{25}Mg T_1 for various ATP concentrations cited. The observed ^{25}Mg spin-lattice relaxation times were almost field independent. This could be explained by the fact that the reorientational modulation of quadrupolar interaction is much slower than the Larmor precession frequency (cf. Table 2). The T_1 minimum that occurred around 290 K corresponded to a value of $\omega_0\tau_s = 0.133$. From the simulation it was found that the $\omega_0\tau_s$ values corresponding to T_1 minimum varied with the exchange rate. The usual way to use $\omega_0\tau \sim 1$ to estimate T_1 minimum was no longer valid for the exchange system. As shown in Figs. 4 and 5 the general trend for the variation of line width with temperature is the same for all samples. On the low temperature side, the increase of line width with temperature indicates that the gradual mixing of the slow component with the fast component through exchange until reaching the

maximum width the and then the effect of motional narrowing appears with increasing temperature. In contrast to field-independent T_1, the result for the field-dependent line widths reflects a larger chemical shift separation of spectral lines at high field.

The correlation time for the fluctuation of electric field gradient at the slow site is mainly dependent on the molecular reorientation. Within the present scope of quadrupolar relaxation, there is no way to distinguish two separate motional correlation times as used in the anisotropic diffusion model.[31] Hence, the obtained reorientational correlation time τ_s can be related to the effective molecular radius using the Debye equation,

$$\tau_s = \frac{4\pi r^3 \eta}{3kT} \tag{14}$$

where k is the Boltzmann constant, r is the effective hydrodynamic radius of Mg^{2+}- ATP complex and η is the solution viscosity. The bulk viscosity at various temperatures may be found in Table 2. The plot of τ_s versus η/T is displayed in Fig. 6. From the slope of linear regression result we calculate that r is 0.72 nm. It represented an effective radius of the complex. Further, the plot of τ_f versus η/T yields r = 0.13 nm. It is about the radius of a water molecule. The tumbling-like motion of water molecules in the hydration layer of Mg^{2+} ion may be accounted for by the fluctuation of electric field gradient at ^{25}Mg nuclei of free ions.

The criterion for fast exchange requires $\delta \cdot \tau_{ex} \equiv \delta \cdot P_f / k_{sf} << 1$ where $\delta \equiv |\delta_s - \delta_f|$. In sample A (C_{Mg} = 100 mM and C_{ATP} = 40 mM) $k_{-1} = k_{sf}$ = 643 s^{-1} it corresponds to a value of $\delta \cdot \tau_{ex} \approx 1.8$ while at 320 K we obtain k_{-1} = 10000 s^{-1} and $\delta \cdot \tau_{ex} \approx 0.12$. Therefore, in the temperature range studied here the system is in the intermediate exchange region.

In accordance with ^{31}P chemical shift studies it was concluded that in aqueous solution with ATP concentrations above 10 mM, the Mg^{2+}-ATP complex exists as aggregates. Below this concentration the aggregate dissociates.[4] It is observed that the changes in chemical shift of ^{31}P with different ATP concentrations studied here are within 15 Hz. The variation of chemical-shift-anisotropy interaction with ATP concentration may not account for the cause of differences in relaxation rates. As cited in Table 3. the dependence of ^{31}P T_1 upon ATP concentration is also evident for the presence of ATP aggregation. In view of the good fit of our model to the relaxation data virtually all the samples with various ATP concentrations share the same τ_s. The value of effective radius of the complex obtained from the Debye equation suggests that the aggregation of ATP moieties has no significant influence on the ^{25}Mg quadrupolar relaxation. Furthermore, with variation of ATP concentrations, the presence of Mg^{2+} causes 10~15% decrease in ^{31}P relaxation in comparison with the corresponding solutions without the Mg^{2+} ion. Since ^{31}P relaxation is in the motional narrowing region as shown in Table 3, it indicates that the extent of aggregation becomes less effective and the ATP moieties become more flexible upon the addition of the Mg^{2+} ion. In the exchange processes, it is believed that the complexation between Mg^{2+} and ATP lessens the interaction in aggregation so that ^{25}Mg relaxation reflects only short-range molecular coupling. Thus, τ_s is not sensitive to the increase of ATP concentration.

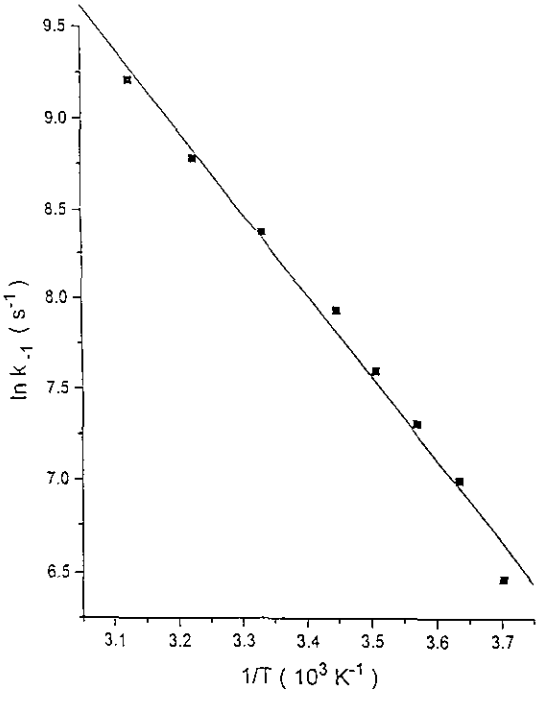

Fig. 7. A logarithmic plot of the dissociation rate constant vs the reciprocal temperature. See text for comparsion of the activation energy obtained in other work.

The dissociation rate constant of the Mg^{2+}-ATP complex as a function of the temperature is shown in Fig. 7. The activation energy can be calculated from the slope in the Arrhenius plot as 8.8 kcal/mol (37 kJ/mol), which agrees

very well with 9.8 kcal/mol found by Sontheimer[3] and 10.0 kcal/mol by Bryant.[6] Also Vasavada[2] found an activation energy of 8.1 kcal/mol with no buffer and Hepes buffer, and 6.8 kcal/mol with Tris buffer.

In the present work ionic strength effects on dissociate rate were expected to be significant. At 25℃, Vasavada[2] found that in a Mg^{2+}-ATP system with ionic strength 0.06 m, k_{-1} = 1200 s^{-1}, and Bryant[6] found k_{-1} = 20000 s^{-1} with ionic strength 4.5 m. The ionic strength in the present system is 1.38 m; we obtained k_{-1} = 4300 s^{-1}. The trend with the variation of ionic strengths seemed to be consistent, but no direct quantitative comparison and theoretical estimation could be made here for the present system.

Traditional methods of analyzing quadrupolar relaxation in exchange systems become more complicated as the condition of fast exchange extreme is even further violated. For instance, a value of 260 ppm for chemical shift separation was found by Byrant from a ^{25}Mg NMR study.[6] With this chemical shift separation, the slow component should be resolved from ^{25}Mg spectra. In comparison with previous work, this study presented more detailed results regarding the dynamics and relaxation behavior of the complex. The study clearly demonstrated that analysis of null point spectra provides a convenient and experimentally simple means to study the binding quadrupolar ions in chemical exchange systems and allows more accurate estimates of the relevant relaxation parameters.

ACKNOWLEDGMENT

Support of this work by grants from the National Science Council of the Republic of China is gratefully acknowledged.

Received December 1, 1998.

Key Words

Mg^{2+}; ATP; Complexation; NMR relaxation.

REFERENCES

1. Forsén, S.; Drakenberg, T.; Wennerstrom, H. *Quart. Rev. Biophys.* **1987**, *19*, 83.
2. Vasavada, K. V.; Ray, B. D.; Rao, B. D. N. *J. Inog. Biochem.* **1984**, *21*, 323.
3. Sontheimer, G. M.; Kuhn, W.; Kalbitzer, R. H. *Biochem. Biophys. Res. Commun.* **1986**, *134*, 1379.
4. Glonek, T. *International Journal of Biocheniistry* **1992**, *24*, 1533, and pertinent references therein.
5. Brown, S. G.; Hawk, R. M.; Komoroski, R. A. *J. Inorg. Biochem.* **1993**, *49*, 1.
6. Bryant, R. G. J *Magn. Reson.* **1972**, *6*, 159.
7. Forsén, S.; Lindman, B. *Methods Biocheni. Anal.* **1981**, *27*, 289.
8. Neurohr, K. J.; Drakenberg, T.; Forsén, S. in " NMR of Newly Accessible Nuclei" (Laszlo, P. ed.), Academic Press, New York, **1983**, *2*, 229.
9. Kumaresan, R.; Tufts, D. W. *IEEE Trans. Acoust. Speech Signal Process.* **1982**, ASSP-30, 833.
10. Kumaresan, R.; Tufts, D. W. *IEEE Trans. Aerosp. Electron. Syst.* **1983**, AES-19, 134.
11. Lin, Y. Y.; Ge, N. H.; Hwang, L. P. *J. Magn. Reson.* **1994**, *103*, 1.
12. Lee, T. S.; Hwang, L. P. *J. Magn. Reson.* **1990**, *89*, 51.
13. Price, W. S.; Ge, N. H.; Hwang, L. P. *J. Magn. Reson.* **1992**, *97*, 656.
14. Price, W. S.; Ge, N. H.; Hwang, L. P. *J. Magn. Reson.* **1992**, *98*, 134.
15. Price, W. S.; Hwang, L. P. *J. Chin. Chem. Soc.* **1992**, *39*, 479.
16. Price, W. S.; Ge, N. H,; Hong, L. Z.; Hwang, L. P. *J. Am. Chem. Soc.* **1993**, *115*, 1095.
17. Chang, W. T.; Shen, Z. S.; Price, W. S.; Ge, N. H.; Hwang, L. P. *J. Magn. Reson.* **1994**, *109*, 98.
18. Sanctuary, B. C. *J. Magn. Reson.* **1985**, *61*, 116.
19. Rose, M. E. *Elementary Theory of AngularMomentum;* Wikey: New York, 1957.
20. Brink, D.M.; Satchler, G. R. *Angular Momentum;* University Press: Oxford, 1968.
21. Furó, I.; Halle, B.; Wong, T. C. *J. Chem. Phys.* **1988**, *89*, 5382.
22. Struis, R. P. W. J.; Bleijser, J.; Leyte, J. C. *J. Phys. Chem.* **1989**, *93*, 7932.
23. Einarsson, L.; Weatlund, P. O. *J. Magn. Reson.* **1988**, *79*, 54.
24. Westlund, P. O.; Wennerstr·m, H. *J. Magn. Reson.* **1982**, *50*, 451.
25. *Handbook of Chemistry and Physics*; Weast, R. C., Ed.; CRC Press: Cleveland, OH, **1984.**
26. Hiyama, Y.; Woyciesjes, P. M.; Brown, T. L.; Torchia, D. A. *J. Magn. Reson.* **1987**, *72*, 1.
27. Klaus, W.; Schlichting, I.; Goody, R. S.; Wittinghofer,

A.; Rösch, P.; Holmes, K. C. *Hoppe-Syler's Z. Physiol. Chem.* **1986,** *367,* 781.
28. O'Sullivan, W. J.; Smithers, G. W. *Meth. Enzymol.* **1979,** *63,* 294.
29. Bull, T. E.; Nome, J. E.; Reimarsson, P.; Lindman, B. J. *J. Am. Chem. Soc.* **1978,** *100,* 4643.
30. Rose, M. E.; Bryant, *J. Magn. Reson.* **1978,** *31,* 41.
31. Hwang, J. S.; Mason, R. P.; Freed, J. H. *J. Phys. Chem.* **1975,** *489,* 79.